Icarus **153**, 451–454 (2001)
doi:10.1006/icar.2001.6691, available online at http://www.idealibrary.com on IDEAL®

NOTE

HST/FGS Observations of the Asteroid (216) Kleopatra

P. Tanga[1]

Osservatorio Astronomico di Torino, Strada Osservatorio 20, I-10025 Pino Torinese (TO), Italy
E-mail: tanga@to.astro.it

D. Hestroffer[2] and J. Berthier

IMCCE, UMR CNRS 8028, Observatoire de Paris, 77 Avenue Denfert Rochereau, F-75014 Paris, France

and

A. Cellino, M. G. Lattanzi, M. Di Martino, and V. Zappalà

Osservatorio Astronomico di Torino, Strada Osservatorio 20, I-10025 Pino Torinese (TO), Italy

Received December 18, 2000; revised June 12, 2001

Interferometric observations of asteroid (216) Kleopatra were performed in January 2000 using the Fine Guidance Sensors (FGS) aboard HST. The FGS data obtained clearly suggest that (216) Kleopatra is composed of two lobes in contact, in agreement with the radar data (Ostro *et al.* 2000, *Science* 288, 836–839), and provide more precise constraints on the absolute size of this peculiar object.

Key Words: **asteroids; imaging; binary; interferometry.**

1. Introduction. Present-day asteroids are the outcomes of a complex history of collisional evolution, dating back to the early epochs of the Solar System. It is presently believed that only a few of the largest main belt objects, those having sizes over 300–400 km, are direct survivors of the early population. The rest of the population, including objects having sizes above 100 km, consists of collisional outcomes. In the disruption of objects of 100 km or more, gravitational reaccumulation of the fragments can play an important role, possibly producing bodies shaped as equilibrium figures, according to their angular momentum (Chandrasekhar 1969, Farinella *et al.* 1982).

When the total angular momentum exceeds some limit, determined by the overall density of the object, rotational fission can conceivably take place, producing binary systems with both components of comparable size (Weidenschilling 1980). Subsequent dynamical and collisional evolution of the two components can lead to coalescence into a single, highly elongated body. This mechanism is probably very different compared with that leading to the presence of small satellites like those of (45) Eugenia and (243) Ida.

In recent times, the existence of binary systems has been successfully established by means of ground-based high-resolution observations, as in the case of (90) Antiope (Merline *et al.* 2000).

The Fine Guidance Sensor interferometer aboard the HST (HST/FGS) has been already used in the past to resolve close binaries and the apparent size of evolved stars (see, e.g., Franz *et al.* 1991, Bernacca *et al.* 1993, Lattanzi *et al.* 1997). Therefore it seemed appropriate to use it for high-resolution observations of asteroids, and a proposal was successfully submitted for a binary-search program. Six large asteroids, including (216) Kleopatra, have been selected for this program. They all show large-amplitude photometric lightcurves that could be explained by either very elongated triaxial ellipsoid shapes or by equilibrium binary models (Cellino *et al.* 1985). In this note, we focus on the results obtained for the main-belt asteroid (216) Kleopatra.

Recently, ground-based adaptive optics observations of (216) Kleopatra have produced strong evidence that this object could have a shape composed by two lobes of comparable size (Marchis *et al.* 1999), as previously suspected from several techniques: photometry (see, e.g., Zappalà *et al.* 1980, Weidenschilling 1981, Cellino *et al.* 1985), Doppler-only radar observations (Mitchell *et al.* 1995), and HST/WFPC imaging (Storrs *et al.* 1999). Subsequent radar observations at Arecibo have produced the higest resolution model of Kleopatra's shape available, in which (216) Kleopatra appears to be formed by two lobes connected by a "handle" (Ostro *et al.* 2000). Adaptive optics images have been found to be coherent with this bi-lobed shape (Merline *et al.* 2000).

In the following, we outline the procedure followed to perform the data reduction and to investigate the response of the FGS interferometer in the presence of a close binary or a two-lobe object. Then we present the analysis of the FGS observations and discuss the contribution in defining size and shape of a complex object such as Kleopatra.[3]

2. Observations and reduction. (216) Kleopatra was observed on January 13, 2000, shortly after the successful third servicing mission, with the FGS1R instrument, as part of cycle 7 observing program #7844 (Zappalà *et al.* 1998). The data were secured in TRANS mode with the F583W filter ($\lambda = 583$ nm,

[1] Associate researcher at the IMCCE, Observatoire de Paris, F-75014 Paris, France. Currently at Observatoire de la Côte d'Azur, Laboratoire Cassini UMR 6529/CNRS, B.P. 4229, 06304, Nice cedex 04, France.

[2] Previously invited researcher at the OATo, I-10025 Pino Torinese (TO), Italy.

[3] Based on observations with the NASA/ESA Hubble Space Telescope, obtained at the Space Telescope Science Institute, which is operated by the Association of Universities for Research in Astronomy, Inc. under NASA Contract NAS5-26555.

0019-1035/01 $35.00

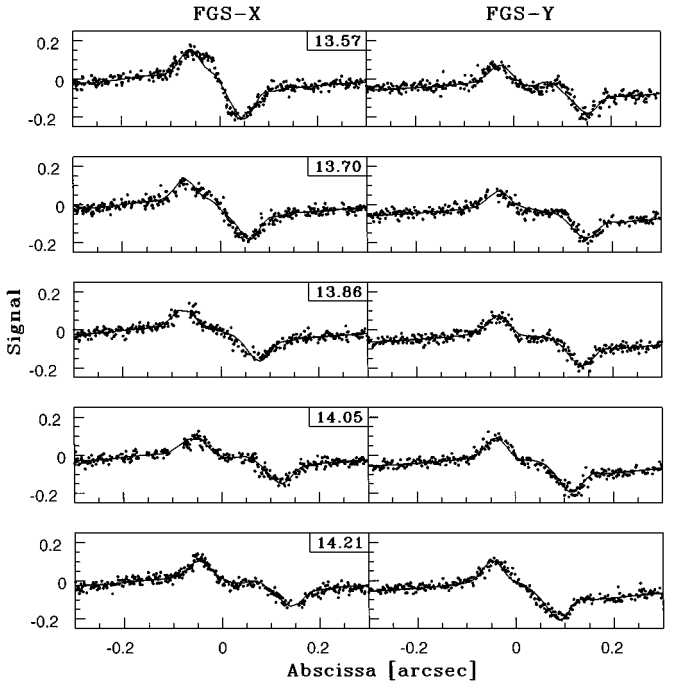

FIG. 1. Observed S-curves for five selected visits on FGS *X* (left panels) and FGS *Y* (right panels). The UTC (hours and decimals) of the observations are given in the small box. The shape of the curve around the origin on FGS *Y* at the first visit is characteristic of an observation of a binary system in which each component is resolved. During the observation, the S-curves change their shape with the rotation of the asteroid. At the last visit the situation is reversed, with the object being better resolved on the FGS *X* direction. The line represents the result of the fit of the two-ellipsoid model as explained in the text.

$\Delta\lambda = 234$ nm) and collection lasted from 13.55 to 14.23 UTC (40.8 minutes).[4] The interferometric response function of the FGS (also called an S-curve from its characteristic shape) refers to the fringe visibility pattern produced by the Koester's prism-based interferometer inside the instrument (Lattanzi *et al.* 1994). To map out the S-curve a full sweep across the target is required. Taking into account pointing uncertainties, the length of the scans was set to 2 arcsec and the sampling step to 1.5 mas.

Each scan produces two interferometric response functions, one for each of the orthogonal FGS axes (identified as FGS *X* and FGS *Y*). Since the target is moving on the sky, the entire observation was divided into 17 "visits." Each visit begins with a target acquisition and recentering and ends with two consecutive scans. This provides two sets of two S-curves; each pair of S-curves is then averaged to improve the S/N ratio. The observational data for a single visit thus correspond to a mean S-curve for each FGS axis. The single-visit coverage of the interferometer (u, v)-plane ((u, v) being the plane of the spatial frequencies resolved by the instrument) is thus limited to two perpendicular segments. Each visit provides information on the shape of the resolved target, as projected on the two FGS axes. However, the asteroid rotated significantly during the observation, causing the S-curves to change with time (Fig. 1). This allowed us to constrain the possible shapes of the target.

As far as this paper is concerned, the most important section of the S-curves in Fig. 1 is the region between the primary (positive and negative) humps. We will show in the following that the structure of the S-curve on this inter-hump interval is the signature of a binary object or, more generally, of a single body whose shape is dominated by two lobes. The modification in time is due to the changing geometry of the object during the observation.

With the orientation of the FGS axis on the sky being known, a modeled response curve can be fitted to each observed S-curve. The model uses a "template" (the observation of a pointlike star of appropriate color) provided by the STScI-FGS team and an assumption on the target size and shape to build a synthetic S-curve. In this analysis, we decided to model the target as a uniform source neglecting, as a first approximation, the effects of albedo inhomogeneities and limb darkening. The synthetic S-curve is obtained by convolving the template with the brightness distribution of the target projected along the scan axis. The projection is the result of the integration of the on-sky brightness distribution of the target along the direction perpendicular to the FGS *X* or FGS *Y* axes.

It is useful to compare the observed S-curves to the simulated signal produced by a single uniform disk. Figure 2 (upper panel) clearly shows that varying the size of a single disk only causes the peak-to-peak amplitude of the S-curve to change; it is not capable of reproducing the features between the two main humps seen in the observed curves.

The lower panel of Fig. 2 shows the synthetic S-curve produced by two close disks of identical brightness and angular extent (fixed at 0.1 arcsec), and whose edge-to-edge separation is made to vary from $sepa = 0.015$ arcsec to $sepa = -0.015$ arcsec (i.e., two partially overlapped disks). The plots clearly show that, as expected, the appearance of the region of the S-curve between the positive and negative maxima is related to the separation of the two components. Of particular interest is the case with negative separation, for this is the only configuration which can explain the lack of secondary humps in some of the observed interferometric traces (Fig. 1). This was the reason we decided to model (216) Kleopatra as a binary object; also, we generalized the three-dimensional shape of the two components to that of uniform brightness ellipsoids. Therefore, the parameters to be derived were the three axis of the two ellipsoids and the separation.

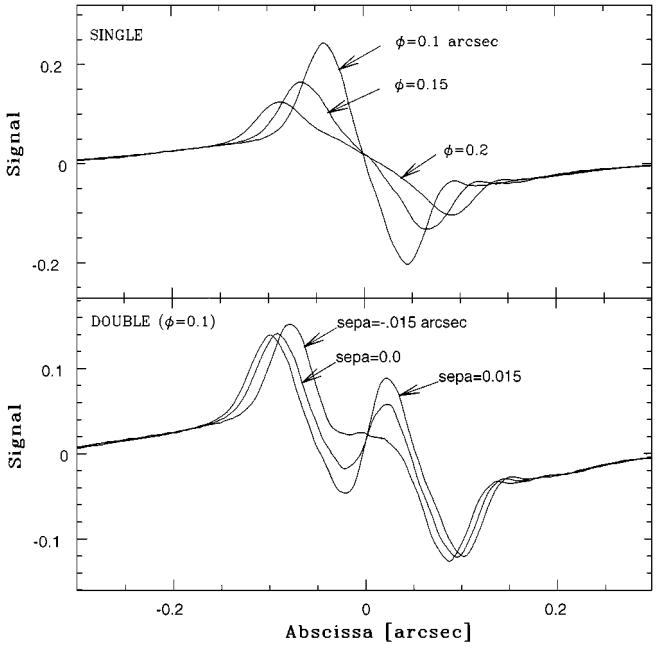

FIG. 2. The upper panel shows the model S-curves for a single ellipsoid of different sizes. While the obtained curves can be compared to some of the scans of Fig. 1, such a simple shape cannot satisfy all of them simultaneously. In the lower panel three S-curves are shown for different separations in the two identical disks model (disk diameter 0.1 arcsec). The curve with a negative separation represents the case of a bi-lobated shape. The direction of the pair is parallel to the scan axis.

[4] See the Web site http://www.stsci.edu/instruments/fgs/ for technical details and the instrument handbook.

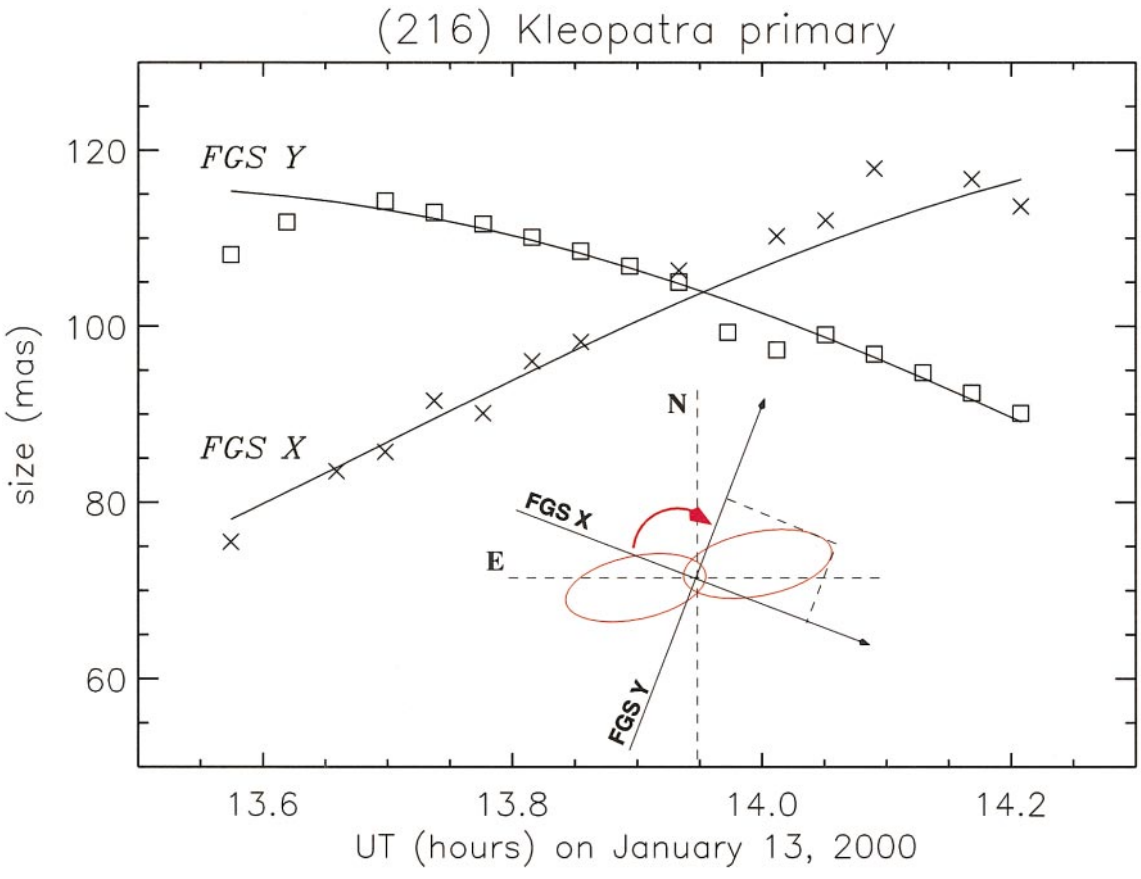

FIG. 3. Variation in time of the size of the asteroid projected on the axis FGS *X* (crosses) and FGS *Y* (boxes). Each symbol correspond to an HST "visit." Some scans were discarded due to strongly degraded data. The orientation on the sky of the two-ellipsoids model (at the epoch of the last visit) is represented in the inset. The aspect angle was 33°.8. The directions on the sky of the FGS *X* and FGS *Y* axis are shown.

The information to constrain the parameters of (216) Kleopatra is provided by the several FGS scans available. In fact, the projections of the assumed shape on the plane normal to the line of sight have to be consistent with all the interferometric curves[5] observed at the times the visits were executed.

The derivation of the best-fit model followed an iterative scheme. To initialize the procedure, independent least-squares fits were done for each visit and separately for each of the two FGS (FGS *X* and FGS *Y*) axes. From these fits, and the FGS orientation data, we derived the projected sizes of both the primary and secondary components of (216) Kleopatra as functions of time (an example for the primary companion is provided in Fig. 3). We then searched for that set of values of the shape parameters (the semi-axis of both ellipsoids) common to all of the scans which minimized, when projected on the FGS axes (the solid curves in Fig. 3), the residuals to the values derived from the individual solutions. At this stage we also adjusted for the rotational phase, searching around the value derived from the photometric curves in Lagerkvist *et al.* (1987–1996). With the shape parameters fixed, the least-squares adjustments to the individual scans were repeated, allowing only the separation to vary. An updated series of projected sizes is thus derived and the next iteration is performed. The whole procedure is repeated until the iterative process converges. The iteration was ended when the rms residual between the computed and the observed curves reached a value comparable to the typical noise of the observed S-curves ($\sim 1.5 \times 10^{-2}$ in the nondimensional units of the S-curves values). The separation of the two ellipsoids was estimated by averaging the values derived from the final fits of the individual S-curves.

[5] Notice that the orientation of the FGS axes was not changed during the different visits.

The adjustment procedure above requires the assumption of the pole direction at the epoch of the observations. We used the average values ($\lambda = 72°; \beta = 16°$) published in Magnusson (1990). Note that our final fit is not very sensitive to the exact pole position, and thus we are not able to constrain it to better then the accuracy of the literature values available ($\sim 10°$).

3. Discussion. The results of our best-fit procedure are listed in Table I. They refer to a binary asteroid made of two ellipsoids whose center-to-center distance is smaller than the sum $a + a'$ of the two semi-major axes (see the inset in Fig. 3). Due to the complexity of the two-step fitting process, it is rather difficult to carry out a careful estimation of the actual uncertainty affecting each parameter. Therefore, approximate estimates of the errors were obtained

TABLE I
Nominal Sizes and Physical Parameters for the Triaxial Ellipsoids Model of Uniform Brightness

Primary			Secondary			Separation	
a	*b*	*c*	*a′*	*b′*	*c′*	*d*	
69	34	16	65	32	23	114	(mas)
75.9	37.4	17.6	71.5	35.2	25.3	125.4	(km)

Note. Data were fitted with a sensitivity of 1 mas. The formal precision is about 2 mas, except for *c* and *c′*, which are approximate estimates (see text).

by searching, independently for each parameter, the range of values in which the fit residuals cannot be distinguished from those of the best-fit solutions. The calculations yielded error estimates of about 2 mas (2.8%) for the a and b axes and a somewhat larger value of $\sim$5 mas (25%) for the minor axis c. This larger error for c indicates the lack of sensitivity on this axis due to the nearly pole-on geometry of the asteroid during the observation (sub-Earth latitude -43°). The estimate of the error on the separation is 5 mas.

Even if the derived uncertainties are optimistic, they clearly show that, when the orientation of the object in space is well defined, the FGS astrometer is capable of giving very accurate size determinations.

Although small, the residuals of the fits to the S-curves of a few initial visits show a trend, like that seen at $x \simeq -0.025$ of the FGS X S-curve taken at 13.57 UTC. This fact suggests that shape and/or albedo departures from the adopted shape are being detected during portions of the observations. It is thus clear that taking into account additional effects (such as small-scale irregularities, albedo markings, and limb darkening) could account for and improve our knowledge of the object, but this would require additional parameters that would be very difficult to meaningfully constrain given the limited coverage of the (u, v)-plane of the FGS data. Consequently, the very small errors quoted for the shape parameter (with the exception of c and c' noted above) represent formal precisions relative to the adopted model.

In summary, among the large variety of models composed by simple forms, only a two-lobed shape—whose components are individually resolved—reproduces the characteristic S-curves observed here. Thus, our HST interferometric observations do confirm that the asteroid (216) Kleopatra has a bi-lobated, nonconvex shape. As for the model adopted, the two-ellipsoids model is close to the equilibrium figures of rotating asteroids proposed by Leone *et al.* (1984). The model, with overall size of 273 km $\times$ 75 km $\times$ 51 km, is more elongated than that based on radar observations proposed by Ostro *et al.* (2000) but still compatible given the uncertainties ($\sim$15 km on the elevation of each surface element and $\sim$25% on the absolute size) quoted in that paper.

Finally, this work demonstrates for the first time that the HST/FGS interferometer is capable of investigating asteroid size and shape. Precise estimates of related quantities require repeated visits over a time interval sufficiently long (as compared to the rotation period) for exploiting the asteroid's changing geometry.

ACKNOWLEDGMENTS

We thank the FGS team at STScI, in particular E. Nelan and D. C. Taylor for their work during the preparation and the execution of the observations. F. Guglielmetti and D. Loreggia were of great help during the data reduction.

REFERENCES

Bernacca, P., M. G. Lattanzi, B. Bucciarelli, U. Bastian, G. Barabaro, R. Pannunzio, M. Badiali, D. Cardini, and A. Emanuele 1993. Hubble Space Telescope astrometric observations of pre-main sequence stars for the HIPPARCOS program. *Astron. Astrophys.* **278**, L47–50.

Cellino, A., R. Pannunzio, V. Zappalà, P. Farinella, and P. Paolicchi 1985. Do we observe light curves of binary asteroids? *Astron. Astrophys.* **144**, 355–362.

Chandrasekhar, S. 1969. *Ellipsoidal Figures of Equilibrium.* Yale University Press, New Haven.

Farinella, P., P. Paolicchi, and V. Zappalà 1982. The asteroids as outcomes of catastrophic collisions. *Icarus* **52**, 409–433.

Franz, O. G., T. J. N. Kreidl, L. H. Wasserman, A. J. Bradley, G. F. Benedict, P. D. Hemenway, W. F. Jefferys, B. McArthur, J. E. McCartney, E. Nelan, P. J. Shelus, D. Story, A. L. Whipple, R. L. Duncombe, L. W. Fredrick, and W. F. Van Altena 1991. Binary star observations with the Hubble Space Telescope fine guidance sensors. *Astrophys. J.* **377**, L17–20.

Lagerkvist, C.-I., P. Magnusson, I. Belskaya, J. Piironen, J. Warell, and M. Dahlgren 1987–1996, *Asteroid Photometric Catalogue* (and updates). Consiglio Nazionale delle Ricerche, Rome.

Lattanzi, M. G., J. L. Hershey, R. Burg, L. G. Taff, S. T. Holfeltz, B. Bucciarelli, I. N. Evans, R. Gilmozzi, J. Pringle, and N. R. Walborn 1994. Hubble Space Telescope fine guidance sensor interferometric observations of the core of 30 Doradus. *Astrophys. J.* **427**, L21–24

Lattanzi, M. G., U. Munari, P. A. Whitelock, and M. W. Feast 1997. Interferometric angular diameters of Mira variables with the Hubble Space Telescope. *Astrophys. J.* **485**, 328–332.

Leone, G., P. Paolicchi, P. Farinnella, and V. Zappalà 1984. Equilibrium models of binary asteroids. *Astron. Astrophys.* **140**(2), 265–272.

Magnusson, P. 1990. Spin vectors of 22 large asteroids. *Icarus* **85**, 229–240.

Marchis, F., D. Hestroffer, A. Cellino, P. Tanga, and V. Zappalà 1999. (216) Kleopatra. IAU *circ.* 7308.

Merline, W. J., L. M. Close, J. C. Shelton, C. Dumas, F. Menard, C. R. Chapman, D. C. Slater, and W. M. Keck II Telescope 2000. Satellites of Minor Planets. IAU *circ. 7503*.

Mitchell, D. L., S. J. Ostro, K. D. Rosema, R. S. Hudson, D. B. Campbell, J. F. Chandler, and I. I. Shapiro 1995. Radar observations of asteroids 7 Iris, 9 Metis, 12 Victoria, 216 Kleopatra, and 654 Zelinda. *Icarus* **118**, 105–131.

Ostro, S. J., R. S. Hudson, M. C. Nolan, J. L. Margot, D. J. Scheeres, D. B. Campbell, C. Magri, J. D. Giorgini, and D. K. Yeomans 2000. Radar observations of asteroid 216 Kleopatra. *Science* **288**, 836–839.

Storrs, A., B. Weiss, B. Zellner, W. Burleson, R. Sichitiu, E. Wells, C. Kowal, and D. Tholen 1999. Imaging observations of asteroids with Hubble Space Telescope. *Icarus* **137**, 260–268.

Weidenschilling, S. J. 1980. Hektor—Nature and origin of a binary asteroid. *Icarus* **44**, 807–809.

Weidenschilling, S. J. 1981. How fast can an asteroid spin? *Icarus* **46**, 124–126.

Zappalà, V., F. Scaltriti, P. Farinella, and P. Paolicchi 1980. Asteroidal binary systems—Detection and formation. *Moon Planets* **22**, 153–162.

Zappalà, V., P. Tanga, A. Cellino, M. Di Martino, and M. G. Lattanzi 1998. A search for main-belt binary asteroids. *HST Progr.* 7488.